

Temperature dependent photoluminescence of organic semiconductors with varying backbone conformation

S. Guha ¹, J. D. Rice¹, Y. T. Yau ¹, C. M. Martin², M. Chandrasekhar²,
H.R. Chandrasekhar², R. Guentner³, P. Scanducci de Freitas³ and U. Scherf³

¹Department of Physics, Astronomy and Materials Science,
Southwest Missouri State University, Springfield MO 65804 USA*

²Department of Physics, University of Missouri, Columbia, MO 65211 USA and

³Institut für Chemie und Polymerchemie, Universität Potsdam, Germany
(Dated: May 29, 2018)

We present photoluminescence studies as a function of temperature from a series of conjugated polymers and a conjugated molecule with distinctly different backbone conformations. The organic materials investigated here are: planar methylated ladder type poly *para*-phenylene, semi-planar polyfluorene, and non-planar *para* hexaphenyl. In the longer-chain polymers the photoluminescence transition energies blue shift with increasing temperatures. The conjugated molecules, on the other hand, red shift their transition energies with increasing temperatures. Empirical models that explain the temperature dependence of the band gap energies in inorganic semiconductors can be extended to explain the temperature dependence of the transition energies in conjugated molecules.

PACS numbers: 78.55Kz, 68.60Dv, 42.70Jk

I. INTRODUCTION

Conjugated organic molecules such as short-chain oligomers and longer-chain polymers are very promising active materials for low-cost, large-area optoelectronic and photonic devices.¹ Semiconducting properties are defined by the ability of these materials to efficiently transport charge (holes or electrons) along the chain due to their π -conjugation or between adjacent chains due to the π -orbital overlap of neighboring molecules. Devices such as organic light-emitting diodes (OLEDs), transistors, and photodiodes are currently attracting much attention. Blue electroluminescent materials are of particular interest for organic displays since blue light can easily be converted into red and green by color-changing media (fluorescent dyes). Commercial availability of organic light-emitting diodes has attracted growing attention to π -conjugated molecules such as pentacene, oligothiophene, oligomers of poly *para*-phenylene (PPP) and polymers^{2,3} such as poly *para*-phenylene vinylene(PPV), polythiophene and PPP. In recent years polyfluorenes (PF) have emerged as attractive alternatives, showing the highest photoluminescence quantum efficiency (55%) compared to other conjugated polymers/molecules in solid state⁴ and also maintain a high hole mobility at room temperature.⁵ Since high photoluminescence quantum yield (PLQY) is the primary consideration in devices such as OLEDs, mechanisms that change the PLQY are crucial to the understanding and design of these devices. Optical processes that reduce the PLQY include competing non-radiative processes, transitions that depopulate the ground state due to reabsorption of photons from singlet states, or situations that can involve intermolecular interactions.

The temperature dependence of electronic states in inorganic semiconductors and heterostructures has been studied extensively in the last 30 years or so. In these

systems the band gaps exhibit large shifts and lifetime induced broadenings as a function of temperature.⁶ One of the first empirical models to explain the temperature dependence of the band gap energy in bulk semiconductors was put forward by Varshni.⁷ Subsequently, there have been other empirical models taking into account an average Bose-Einstein statistical factor for phonons to explain the temperature dependence of the electronic states.^{8,9} This latter model fits the temperature dependence of the transition energies better in narrow-well inorganic semiconductor heterostructures and superlattices.¹⁰

In inorganic semiconductors the two mechanisms that are responsible for the temperature dependence of energy bands at constant pressure are thermal expansion and renormalization of band energies by electron-phonon interactions. Typically the former mechanism has a negligible effect so that the changes in the band gap energies arise primarily from electron-phonon interactions. Theoretical calculations of the temperature dependence of band energies in Si and Ge that take into account such electron-phonon interactions agree very well with the experimental results.¹¹

The motivation of this work is to understand the temperature dependence of the electronic states in organic semiconductors using steady state photoluminescence (PL) spectroscopy and to test the extension of the existing models for inorganic semiconductors to organic materials. We compare different conjugated materials, namely long-chain polymers and short-chain oligomers with distinct conformational variations in their backbone.

Spectroscopic properties of conjugated molecules and polymers are highly sensitive to changes in backbone conformation. The three families of conjugated materials that we compare in this work have distinct differences in their backbone conformation. They include planar methyl substituted ladder-type poly

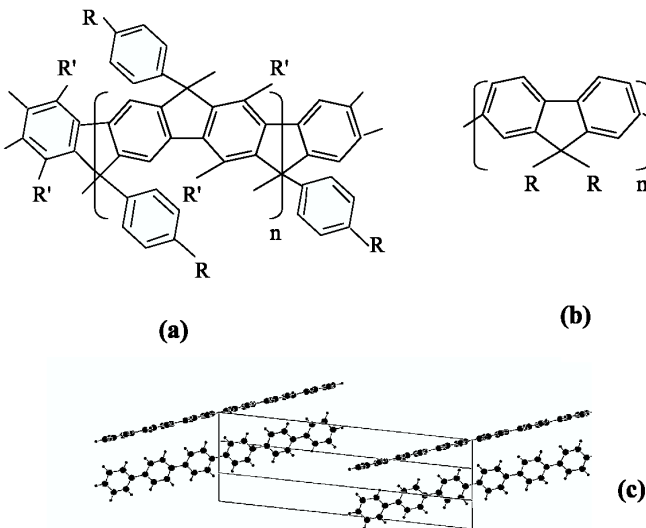


FIG. 1: Chemical structure of (a) MeLPPP (b) PF2/6 and (c) PHP. In (a) R and R' refer to $C_{10}H_{21}$ and C_6H_{13} , respectively and in (b) R refers to the ethyl hexyl side chain.

para-phenylene (MeLPPP), semi-planar poly[2,7-(9,9'-bis(2-ethylhexyl)fluorene (PF2/6) and non-planar (*para* hexaphenyl) (PHP). All three materials are of technological importance due to their strong blue luminescence and high chemical purity. They have been used as active materials in OLEDs.^{4,12,13} Both MeLPPP and PF2/6 are long-chain processable conjugated polymers¹⁴ whereas PHP is a short-chain oligophenyl that forms monoclinic crystallites of space group $P2_1/a$.¹⁵

PHP is characterized by a torsional degree of freedom between neighboring phenyl rings. In the crystalline state the molecules are arranged in layers, with a herringbone type arrangement found in each layer as shown in Fig. 1(c). PHP can be planarized by the application of hydrostatic pressure.¹⁶ On the average, at room temperature it is more planar than at lower temperatures. MeLPPP is amorphous due to the bulky side groups. Neighboring phenyl rings are planar due to the methyl bridges and show no torsional degree of freedom (see Fig. 1(a)). The planarity between phenyl rings results in a high intrachain order and a low defect concentration. This is attributed to the synthesis method, which is highly selective in forming only certain bonds, and hence reduces the number of defects.¹⁷

PF2/6, on the other hand, can be viewed as a semi-planar polymer. It forms planar monomer units but has a torsional degree of freedom between adjacent monomer units as shown in Fig. 1(b). The alkyl side chains of the fluorene moieties have been shown to strongly influence the solid-state packing of the molecule.¹⁸ We also compare the spectra of two other derivatives of PF: a dialkylated copolymer, poly[9,9-bis(3,7,11-trimethyldodecyl)fluorene-2,7-diyl] (PF1112)

and poly[9,9-bis(4-(2-ethylhexoxy)phenyl) fluorene] (PF-P). The copolymer has longer alkyl side chains compared to PF2/6 with 2% of 2,7-fluorenone units incorporated in the backbone as a model for a photodegeneration-induced defect-rich polyfluorene. PF-P is a diphenyl-substituted PF exhibiting an extraordinarily small defect concentration.

Upon further processing some polyfluorene films display a β phase, which has a more extended intrachain π -conjugation, in addition to the regular glassy α phase. The β phase has been detected in 9,9-di-*n*-octyl-PF (PF8 or PFO) upon thermal cycling from 80 to 300 K¹⁹ and slowly reheating it to room temperature or exposing a film to the vapor of a solvent.²⁰ The β phase shows a distinct red shift of absorption and emission peaks with a well-resolved vibronic progression both in absorption and emission. In contrast, the α phase shows a well-resolved vibronic progression only in the emission spectrum. Using x-ray and electron diffraction measurements, Lieser *et al.* have shown that the β phase is completely absent in PF with branched side groups like PF2/6.²¹

This paper is organized as follows; Section II describes the experimental setup. In Section III, we present the PL results from MeLPPP, PF, and PHP as a function of temperature. Section IV is a discussion of our results, followed by our conclusions in Section V.

II. EXPERIMENTAL DETAILS

Highly purified PHP powder was obtained from Tokyo Chemical Industries Ltd. PL spectra were measured from films of MeLPPP, PF, and PHP. The MeLPPP and PF2/6 films were prepared by spin coating on a glass slide from a toluene solution, and their thickness was 1000 Å. We also prepared a thicker film (30,000 Å) by dropcasting PF2/6. In this paper PF(A) and PF(B) refer to the thicker and thinner PF2/6 films, respectively. The films were dried at room temperature. The PHP film was prepared by vacuum evaporation. PHP was evaporated in high vacuum (10^{-6} mbar) on regular glass substrates. PHP powder was put in a quartz crucible that was heated by passing 73 A of current. The thickness of the sample was 1000 Å. The PL spectra were excited using the 363.8 nm line of an Ar⁺ laser. The luminescence excitation was analyzed with a SPEX 0.85 m double monochromator equipped with a cooled GaAs photomultiplier tube and standard photon counting electronics. The samples were loaded in a cryostat and evacuated to below 100 mTorr to prevent photo-oxidative damage. For low temperature measurements a closed cycle refrigerator was employed.

III. PL RESULTS

A vibronic progression is seen in the PL emission for all the materials under consideration, indicating a coupling of the backbone carbon-carbon stretch vibration to

electronic transitions. The vibronic spacing in all the samples lies between 1300 and 1400 cm⁻¹. The vibronic peaks result from a non-zero overlap of different vibronic wavefunctions of the electronic ground and excited states. The emissive transition highest in energy is called the 0-0 transition, which takes place between the zeroth vibronic level in the excited state and the zeroth vibronic level in the ground state. The 0-1 transition involves the creation of one phonon. In the adiabatic picture, vibronic progression in the electronic spectra implies that the ground and excited state equilibrium structures are displaced relative to one another in configuration space. The spectral intensity is approximated by the superposition of transitions between the vibrational frequencies of the ground- and the excited electronic states. In the emission process the probability of the 0th vibronic excited state to the nth vibronic ground state is given by

$$I_{0 \rightarrow n} = \frac{e^{-S} S^n}{n!} \quad (1)$$

where S , the Huang-Rhys factor, is given by $M\omega/2\hbar(\Delta)^2$.²² Here ω is the vibrational frequency, M is the reduced mass of the harmonic oscillator that couples to the electronic transition and Δ is the displacement of the potential curve between the ground and excited electronic states. The Huang-Rhys factor therefore corresponds to the average number of phonons that are involved when the excited molecule relaxes from its ground state configuration to the new equilibrium configuration in the excited state (after the absorption of a photon) and $S\hbar\omega$ is the relaxation energy. If we assume that ω is the same for ground and excited states and that the potentials are perfectly parabolic, S can be determined from the fractional intensity of the vibronic peaks. In particular,

$$S = (I_{0 \rightarrow 1} + 2I_{0 \rightarrow 2} + 3I_{0 \rightarrow 3})/I_{total} \quad (2)$$

$I_{0 \rightarrow 1}$, $I_{0 \rightarrow 2}$, and $I_{0 \rightarrow 3}$ refer to the intensity of the emission from the zeroth vibrational level excited state to the first, second and third vibrational level of the ground state, respectively. I_{total} is the total intensity of the individual vibronics. Here we assume that the transition matrix elements are the same for all vibronics and neglect all vibronics above 0-3.

A. MeLPPP Film

Figure 2 shows the PL spectra of an MeLPPP film at a few selected values of temperature. The PL spectrum was fitted with Gaussians in order to obtain the individual peak positions, amplitudes and broadening (FWHM) parameters. The three main vibronic peaks observed are labeled as the 0-0, 0-1 and the 0-2. There are additional vibronic peaks observed between the main vibronic peaks that are also seen in other works.²³ The dotted line under the 30 K spectrum is a representative of our fits. At

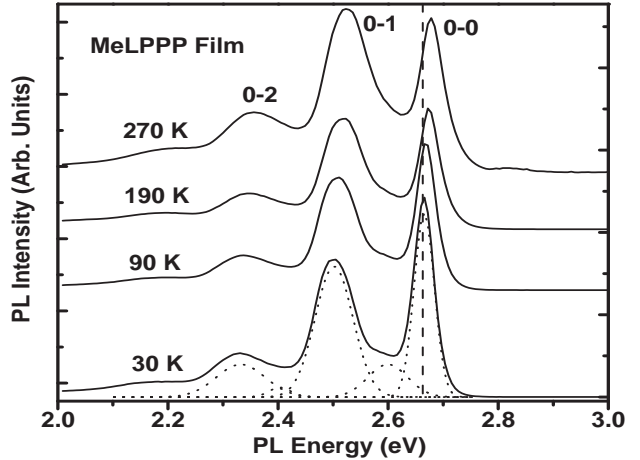


FIG. 2: PL spectra of a MeLPPP film at a few values of temperature. The dotted line under the 30 K data shows the actual fit to the data. The vertical dashed line indicates a blue shift of the 0-0 vibronic peak with increasing temperature.

30 K the main vibronic peaks that are observed are the 0-0 peak at 2.67 eV, the 0-1 at 2.5 eV, 0-2 vibronic peak at 2.33 eV, and the 0-3 peak at 2.19 eV. In addition, vibronic replicas are observed at 2.61 eV and 2.4 eV. The energy difference between the main successive vibronic peaks is 0.17 eV indicative of the coupling of the =C-C=C-C= stretch vibration to the conjugated backbone. At all temperatures the PL spectra were fit with the same number of Gaussian peaks for consistency. The overall spectrum not only blue shifts with increasing temperatures but the relative intensities of the individual vibronic peaks change as well.

Figure 3 (a) shows the energy position of the 0-0 and the 0-1 vibronics as a function of temperature. The 0-2 peak in MeLPPP also shows a similar behavior. The average value of the rate of shift is 7.5×10^{-5} eV/K. Figure 3 (b) shows the FWHM (eV) for the 0-0 and the 0-1 vibronic peaks as a function of temperature. The bold line is a guide to the eye. The line widths decrease till 100 K and then increase beyond 100 K. This cannot be attributed to any fitting artifact: at all temperatures the PL spectrum is fitted with same number of individual vibronic peaks (shown in the 30 K data of Fig. 2) which are allowed to vary in position, amplitude and width till the best fit is obtained. Moreover, both the 0-0 and the 0-1 vibronic peaks show the same trend.

B. PF Film

Figure 4 shows the PL spectra from two PF2/6 films (with different thickness) for a few selected values of temperature. The relative intensity of the 0-0 peak to the 0-1 peak in PF(A) (thicker film) is lower compared to PF(B) (thinner film) indicating a higher self-absorption in PF(A). At 30 K the main vibronic peaks that are observed are the 0-0 peak at 2.93 eV, the 0-1 at 2.77 eV

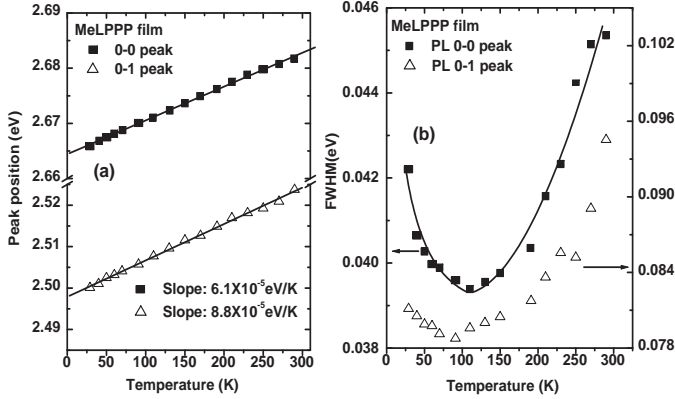


FIG. 3: (a) The peak position of the 0-0 and the 0-1 PL transitions as a function of temperature in MeLPPP (b) FWHM of the 0-0 and the 0-1 peak as a function of temperature in MeLPPP.

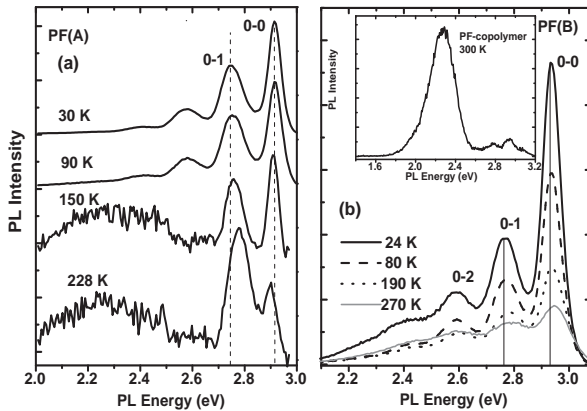


FIG. 4: PL spectrum of PF2/6 at selected values of temperature for a (a) thicker and (b) thinner film. The vertical lines show the shift in the transition energies with temperature. The inset in (b) is the PL spectrum of PF-copolymer at 300 K. The strong 2.3 eV peak is related to the emission from the keto defects.

and the 0-2 transition at 2.59 eV in PF(B). An additional vibronic replica is observed at 2.86 eV between the 0-1 and 0-2 peaks. The PL transition energies show a blue shift with increasing temperatures, similar to the MeLPPP sample. The peak positions and the FWHM of the 0-0 and the 0-1 PL vibronics are shown in Fig. 5. The sublinear behavior of the 0-0 peak position in PF(B) with increasing temperatures may be related to self-absorption effects.

The PL spectra of PF(A) show a slightly different behavior as seen in Fig. 4(a). The 0-0 peak red shifts whereas the 0-1 peak blue shifts with increasing temperatures. The red shift of the 0-0 peak in this sample is most probably an artifact due to self-absorption effects.

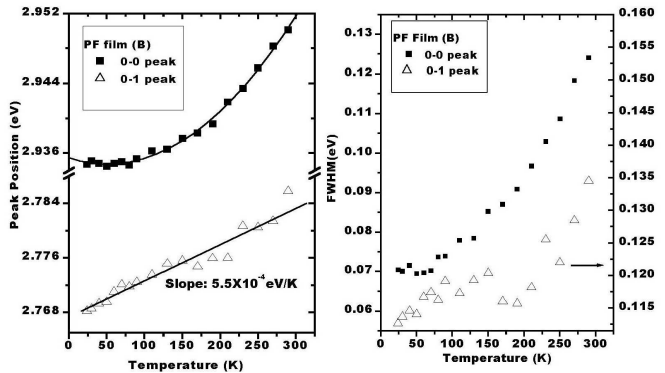


FIG. 5: (a) Peak position of the 0-0 and the 0-1 peak in PF(B) as a function of temperature. (b) FWHM of the 0-0 and the 0-1 peak in PF(B) as a function of temperature.

With increasing temperatures a broad peak at 2.3 eV emerges at around 150 K, shown in Fig. 4(a). Recent work suggests that this peak is related to the emission from keto defects sites (9-fluorenone sites).^{18,24} These defect sites act as guest emitters which can efficiently trap singlet excitons created on the conjugated polyfluorene backbone by a dipole-dipole induced Förster-type energy transfer.²⁵ The keto defect sites can be accidentally incorporated into the π -conjugated PF backbone due to the presence of non-alkylated or monosubstituted fluorene sites during synthesis or as a result of a photo-oxidative degradation process. In order to reduce photodegradation due to the exciting UV, the samples were kept in vacuum during our PL measurements. The concentration of these defect sites is quite low in the PF2/6 sample since the 2.3 eV emission is absent in the thinner PF(B) film. Also, it is a thermally activated process; in PF(A) the defect related emission is only observed for temperatures above 150 K. The inset of Fig. 4 (b) shows the PL spectrum from PF1112, the copolymer with 2% incorporated fluorenone sites. The strong 2.3 eV emission is from the keto defects which overwhelms the emission from the PF backbone.

In contrast, the diphenyl-substituted PF (PF-P) is expected to have almost no keto defects due to a different synthesis of the corresponding monomer blocks that prevents non- or monosubstituted fluorene sites. We compare the temperature dependent PL from a drop-casted film of PF-P to the PF2/6 sample of film thickness comparable to the sample PF(A). Figure 6 (a) shows the PL spectra from PF-P for selected values of temperature. Clearly the 2.3 eV emission is not observed at higher temperatures unlike in PF(A), indicating that the sample is almost free of keto defect sites. Figure 6 (b) shows the peak position of the 0-0 and the 0-1 vibronics as a function of temperature. The average value for the rate of shift of the PL vibronics is $5.2 \times 10^{-5} \text{ eV/K}$.

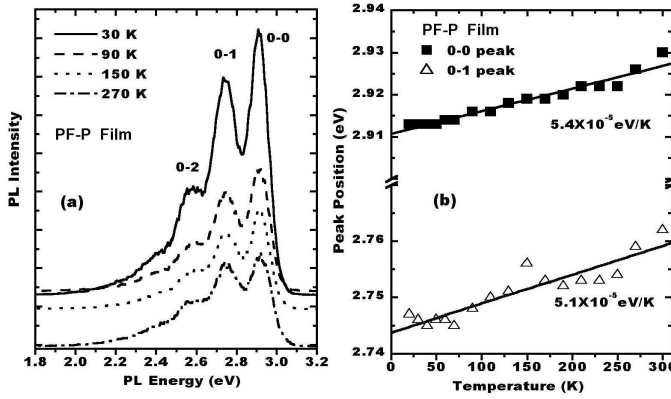


FIG. 6: (a) PL spectra of PF-P at a few values of temperature. (b) The 0-0 and the 0-1 peak position as a function of temperature in PF-P.

C. PHP

The PL measurements from PHP were measured both from the powder and from a thin evaporated film. Figure 7 shows the PL spectra both from the powder and film for selected temperatures. The 0-0 transition is not observed in the powder due to self-absorption. The film also shows a certain amount of self-absorption since the relative intensity of the 0-0 peak is smaller compared to the 0-1 or the 0-2 transition peak. At 30 K the main vibronic peaks that are observed are the 0-0 peak at 3.12 eV, the 0-1 at 2.95 eV and the 0-2 vibronic peak at 2.78 eV. Additional vibronic peaks are observed at 3.07 eV and 2.86 eV. The individual vibronics red shift with increasing temperatures both in the film and powder. A red shift of the PL spectrum with increasing temperatures in PHP has been observed before, but a detailed analysis was not carried out.^{16,26} The PHP film was more prone to local heating effects during the PL measurement; we therefore restrict our analysis to the PHP powder. Figures 8(a) and (b) show the individual positions of the 0-1 and the 0-2 peaks, respectively, from the PHP powder. The bold line is a fit to an empirical model, discussed in detail in Section IV.

IV. DISCUSSION

Conjugated polymers can be viewed as an inhomogeneous collection of varying-length chain segments. Time- and frequency-resolved optical studies show that after a photon excites a chain segment with energy above the threshold, the exciton that is created executes a random walk through the density of states via Förster energy transfer,²⁵ until it becomes trapped on a low-energy site,

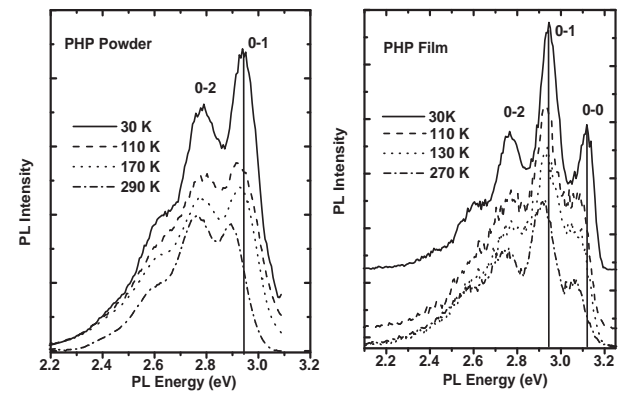


FIG. 7: PL spectra at four selected values of temperature for (a) PHP powder and (b) a thin evaporated PHP film.

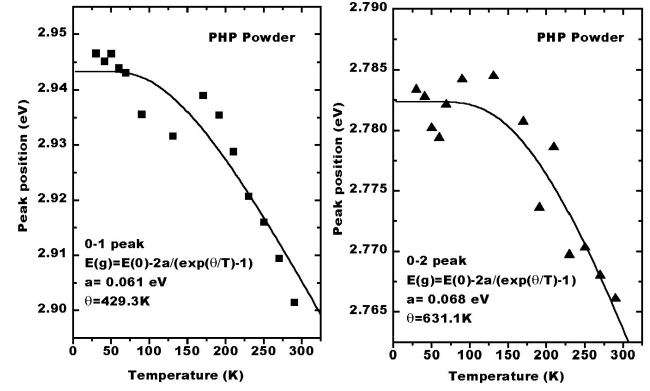


FIG. 8: Peak position of the (a) 0-1 and the (b) 0-2 PL transition energies from PHP powder as a function of temperature. The bold line is a fit to Eq. (3).

from where emission occurs. These sites presumably have a higher conjugation length.^{27,28}

The temperature dependence of the PL energies is different for long-chain conjugated polymers compared to the shorter chain oligomers; conjugated polymers show a blue shift of PL energies with increasing temperatures, whereas conjugated molecules like PHP show a red shift with increasing temperatures. It is interesting to point out that although the two types of polymers studied here have differences in their backbone conformation, MeLPPP being planar and PF2/6 is semi-planar, both show the same trend as a function of temperature. A similar behavior has been observed in other conjugated polymers such as PPV²⁷ and MEH-PPV.^{29,30} Though the general trend in PL energies as a function of temperature is similar in the conjugated polymers investigated

in this work, there are differences in the magnitude of their shifts with increasing temperatures.

The relative strengths of the vibronic transitions also change along with shifts in energy with temperature. The Huang-Rhys factor decreases both for the polymers and PHP with decreasing temperatures, as shown in Fig. 9. The S -factor was calculated using Eq. (2). Smaller molecules exhibit a larger S -factor due to their large normal coordinate displacements. For a detailed explanation see Hagler *et al.*²⁹. It is therefore not surprising that PHP has a higher S -factor compared to the polymers. From Fig. 9 it is seen that PHP shows a saturation effect at higher temperatures. This may be related to the fact that since the electronic transition energies red shift with increasing temperatures, there may be a higher overlap of the 0-0 peak with absorption resulting in a further decrease in the intensity of the 0-0 peak in addition to the effect of temperature. A decrease in S with decreasing temperatures has been observed in other works and is interpreted as an effect arising from increased conjugation due to exciton delocalization.²⁷ This picture by itself cannot explain the temperature dependence of the PL from both the conjugated polymers and the shorter molecules, since PHP clearly shows a blue shift of transition energies with decreasing temperatures. We also observe the PL emission from quaterphenyl powder to blue shift with decreasing temperatures. Therefore we must really look at these systems separately: the conjugated polymers that have a distribution of chain lengths and the shorter molecules that have more or less the same chain length distribution.

The electronic energies in bulk inorganic semiconductors display temperature dependence mainly due to renormalization of band energies by electron-phonon interactions. The temperature dependence of the interband transitions can be described with an expression in which the energy thresholds decrease proportional to the Bose-Einstein statistical factors for phonon emission plus absorption⁸

$$E_g(T) = E(0) - \frac{2a}{[\exp(\Theta/T) - 1]} \quad (3)$$

where $E(0)$ is the band gap energy at 0 K, a is the strength of the exciton-phonon interaction. This includes contribution both from the acoustical and optical phonons. Θ is the average phonon temperature. By fitting the 0-1 and the 0-2 PL vibronics of PHP with Eq. 3 (see Fig. 8), we obtain an average value of the strength of the exciton-phonon interaction as 0.065 eV and the average phonon temperature to be 530 K. These values are comparable to other inorganic semiconductors, for example in bulk GaAs, $a=0.057$ eV and $\Theta=240$ K. The PL linewidth of the individual vibronics in PHP show a scatter with increasing temperature and on the average remains a constant.

Although the polymers, MeLPPP, PF2/6 and PF-P all show a blue shift of their PL energies with increasing temperatures, they shift at different rates. The PL vibronics

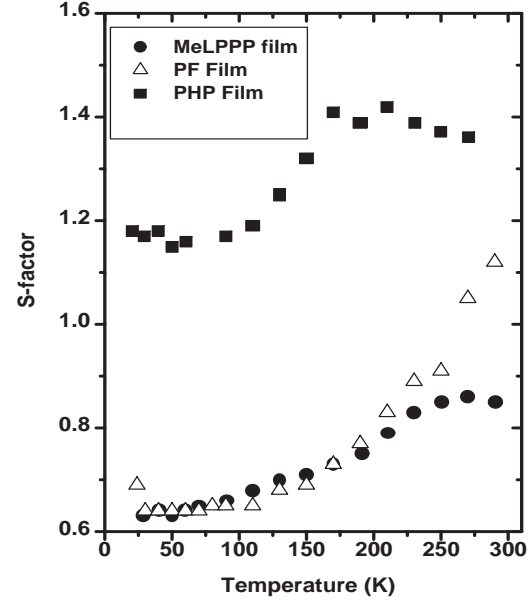


FIG. 9: Huang-Rhys factor versus temperature for MeLPPP, PF and PHP films. S was calculated using Eq. 2

in MeLPPP and PF-P shift at rates of 7×10^{-5} eV/K and 5×10^{-5} eV/K, respectively (Figs. 3(a) and 6(b)). PF2/6, on the other hand, shows a higher shift of the 0-1 PL vibronic peak (55×10^{-5} eV/K) as shown in Fig. 5(a). The different rates have to do with the differences in their conjugation length, especially since their molecular weights are not that different. PF2/6 is a more flexible polymer due to the alkyl substitution unlike MeLPPP and PF-P that have aryl substituents. PF2/6 undergoes some additional geometry changes (higher disorder in the chain) with increasing temperature; the higher rate of the temperature dependence of the PL transitions may be related to these additional disorder processes in the polymer. PF2/6 and PF-P show a broadening of the PL line widths with increasing temperatures. Beyond 100 K, MeLPPP shows a broadening of the PL line widths as seen in Fig. 3 (b).

A red shift of the PL energies with decreasing temperatures from the two families of the conjugated polymers with planar backbone confirmation (MeLPPP) and semi-planar backbone confirmation (PF2/6 and PF-P) confirms Bässler and Schweitzer's²² argument that the process should not really depend upon the freezing out of torsional modes. Otherwise, MeLPPP, which has a planar backbone conformation, should show a different behavior. The shifts in the PL energies reflect more on the temperature dependence of the relaxation process. A plausible explanation is that upon increasing the temperature, the excitons that are created on the polymer backbone do not easily migrate to the low energy segments; they remain localized on the shorter chain segments that have higher energies.

In PHP the main contribution to the temperature dependence of electronic energy arises from the exciton-phonon interaction term, similar to that in inorganic

semiconductors. A possible scenario is that in the longer chain polymers both renormalization of band energies due to electron-phonon interaction as well as prevention of energy migration to lower energy sites play a role, and the latter appears to be dominant.

It is interesting to point out that in inorganic semiconductors such as GaN quantum dots (QDs), PL energies blue shift with increasing temperatures, similar to the conjugated polymers.³¹ This is in contrast to bulk GaN,³² where the band energies red shift with increasing temperatures. In the quantum dot system since there is a distribution of the size of the dots; increasing temperatures result in a preferential loss of carriers from larger QDs (which have lower energies), resulting in a net blue shift of the transition energy due to the emission from the smaller dots.

V. CONCLUSION

We have presented a systematic temperature dependent steady-state PL studies from a series of conjugated polymers and a molecule with variations in their backbone conformations. The conjugated polymers show a blue shift of their PL transition energies with increasing temperature, independent of their actual backbone conformation. MeLPPP, which is planar and PF that has a

semi-planar backbone confirmation show a similar trend in their PL energies as a function of temperature. The shifts in the electronic energies reflect on the temperature dependence of the actual relaxation process whereby the migration of excitons to the longer chain segments is hampered with increasing temperatures.

The shorter conjugated molecule, PHP, which has a similar distribution of chain lengths, shows the opposite trend: a red shift of the transition energies with increasing temperature, indicating a renormalization of band energies due to electron-phonon interaction. This behavior is similar to that observed in bulk inorganic semiconductors and can be described by an empirical model that takes into account the Bose-Einstein statistical factors for phonon emission and absorption.

Acknowledgments

Work at SMSU was partly funded by an award from the Research Corporation #CC5332 and the Petroleum Research Fund #35735-GB5. S.G. would also like to acknowledge the SMSU summer faculty fellowship. U.S. thanks SONY International Europe, Stuttgart, and the Deutsche Forschungsgemeinschaft (DFG) for financial support.

* E-mail: sug100f@smsu.edu

¹ For a review see *Organic electronics: introduction*, J.M. Shaw and P.F. Seidler, IBM J. Res. & Dev. **45**, 3 (2001); *Handbook of Conducting Polymers*, edited by T.A. Skotheim, R.L. Elsenbaumer and J.R. Reynolds, Marcel Dekker, Inc. (1997).

² J.H. Burroughes, D.D. C. Bradley, A.R. Brown, R.N. Marks, K. Mackay, R.H. Friend, P.L. Burns, A.B. Holmes, Nature **347**, 539 (1990).

³ Y. Ohmori, M. Uchida, K. Muro, K. Yoshini, Jpn. J. Appl. Phys. **30**, L1938 (1989).

⁴ A.W. Grice, D.D. C. Bradley, M.T. Bernius, M. Inbasekaran, W.W. Wu, and E.P. Woo, Appl. Phys. Lett. **73**, 629 (1998).

⁵ M. Redecker, D.D.C. Bradley, M. Inbasekaran, and E.P. Woo, Appl. Phys. Lett. **73**, 1565 (1998).

⁶ See, for example, S. Adachi, *GaAs and Related Materials: Bulk Semiconducting and Superlattice Properties* (World Scientific, Singapore, 1994).

⁷ Y.P. Varshni, Physica **34**, 149 (1967).

⁸ L. Vina, S. Logothetidis, and M. Cardona, Phys. Rev. B **30**, 1978 (1984).

⁹ P. Lautenschlager, M. Garriga, S. Logothetidis, and M. Cardona, Phys. Rev. B **35**, 9174 (1987).

¹⁰ S. Guha, Q. Cai, M. Chandrasekhar, H.R. Chandrasekhar, H. Kim, A.D. Alvarenga, R. Vogelgesang, A.K. Ramdas, and M.R. Melloch, Phys. Rev. B **58**, 7222 (1998).

¹¹ P. Lautenschlager, P.B. Allen and M. Cardona, Phys. Rev. B **31**, 2163 (1985).

¹² S. Tasch, A. Niko, G. Leising, and U. Scherf, Appl. Phys.

Lett. **68**, 1090 (1996).

¹³ S. Tasch, C. Brandstätter, F. Meghdadi, G. Leising, L. Athouel, and G. Froyer, Adv. Mat. **9**, 33 (1997).

¹⁴ S. Setayesh, D. Marsitzky, and K. Müllen, Macromolecules **33**, 2016 (2000).

¹⁵ K.N. Baker, A.V. Fratini, T. Resch, H.C. Knachel, W. W. Adams, E. P. Soccia, and B.L. Farmer, Polymer **34**, 1571 (1993).

¹⁶ S. Guha, W. Graupner, R. Resel, M. Chandrasekhar, H.R. Chandrasekhar, R. Glaser, and G. Leising, Phys. Rev. Lett. **82**, 3625 (1999).

¹⁷ J. Grimme, M. Kreyenschmidt, F. Uckert, K. Müllen, and U. Scherf, Adv. Mater. **7**, 292 (1995).

¹⁸ U. Scherf and E.J.W. List, Adv. Mater. **14**, 477 (2002).

¹⁹ A.J. Calby, P.A. Lane, H. Mellor, S.J. Martin, M. Grell, C. Giebeler, D.D.C. Bradley, M. Wohlgemant, C. An, and Z.V. Vardeny, Phys. Rev. B **62**, 15604 (2000).

²⁰ M. Grell, D.D.C. Bradley, X. Long, T. Chamberlain, M. Inbasekaran, E.P. Woo, and M. Soliman, Acta Polym. **49**, 439 (1998).

²¹ G. Lieser, M. Oda, T. Miteva, A. Meisel, H.-G. Nothofer, U. Scherf, and D. Neher, Macromolecules **33**, 4490 (2000).

²² H. Bässler, and B. Schweitzer, Acc. Chem. Res. **32**, 173 (1999).

²³ E.J.W. List, C. Creely, G. Leising, N. Schulte, A.D. Schlüter, U. Scherf, K. Müllen, and W. Graupner, Chem. Phys. Lett. **325**, 132, (2000).

²⁴ E.J.W. List, R. Guentner, P. S. de Freitas, and U. Scherf, Adv. Mater. **14**, 374 (2002).

²⁵ T. Förster, Ann. Phys. **2**, 55 (1948).

²⁶ A. Piaggi, G. Lanzani, G. Bongiovanni, A. Mura, W. Graupner, F. Meghdadi, G. Leising, and M. Nisoli, Phys. Rev. B **56**, 10133 (1997).

²⁷ S-H Lim, T.G. Bjorklund, C. J. Bardeen, Chem. Phys. Lett. **342**, 555 (2001).

²⁸ R. Kersting, B. Mollay, M. Rusch, J. Wenisch, G. Leising, and Kauffmann, J. Phys. Chem. **106**, 2850 (1997).

²⁹ T. W. Hagler, K. Pakbaz, K.F. Voss, and A.J. Heeger, Phys. Rev. B **44**, 8652 (1991).

³⁰ A.K. Sherdian, J.M. Lupton, I.D.W. Samuel, and D.D.C. Bradley, Chem. Phys. Lett. **322**, 51 (2000).

³¹ J. Brown, C. Elsass, C. Poblenz, P.M. Petroff, and I.S. Speck, Phys. Stat. Sol (B) **228**, 199 (2001).

³² C.F. Li, Y.S. Huang, L. Malikova, and F.H. Pollak, Phys. Rev. B **55**, 9251 (1997).